Full Paper: Copolymer $S_{13}E_{60}$ (E = oxyethylene unit, S = oxyphenylethylene unit) was synthesised and characterised by gel permeation chromatography (for distribution width) and ^{13}C NMR spectroscopy (for absolute molar mass and composition). Dynamic and static light scattering were used to determine micellar properties in dilute aqueous solution at three temperatures (20, 30 and 40 °C): i.e. association number, hydrodynamic and thermodynamic radii. Comparison with reported results for related copolymers allowed exploration of the dependence of these properties on hydrophobe block length. The phase behaviour of the copolymer in aqueous solution was defined using tube inversion and rheometry (for yield stress and dynamic modulus). The hard-gel boundary was detected by both methods in satisfactory agreement. Discussion is focused on effects of micelle stability on the shape and extent of the hard-gel region of the phase diagram. A region of soft gel was detected at low concentrations by rheometry, and assigned to a percolation mechanism.

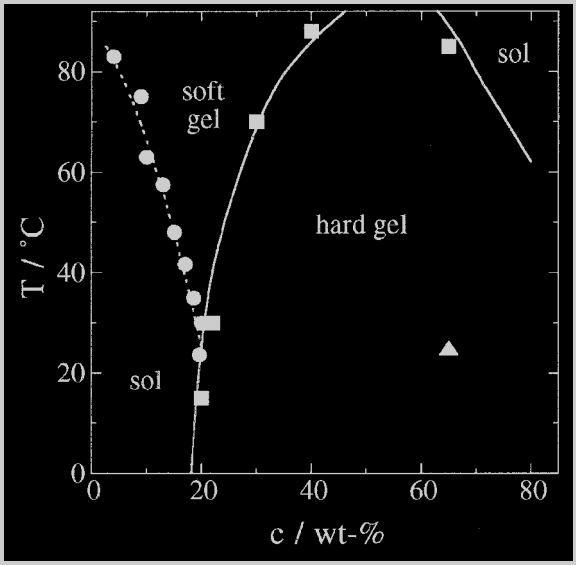

Phase diagram for aqueous solutions of copolymers $S_{13}E_{60}$. The solid curve is that defined for hard gel taken from Figure 4. Data points (●) and the dotted curve indicate the sol/soft-gel boundary; data points (■) indicate the temperatures at which the storage and loss moduli fell sharply to reach a low value, giving a coincident definition of the hard-gel boundary; data point (▲) indicates the temperature of a transition within the hard-gel region.

Association Properties of a Diblock Copolymer of Ethylene Oxide and Styrene Oxide in Aqueous Solution Studied by Light Scattering and Rheometry

Antonis Kelarakis,[1] *Vasiliki Havredaki,*[1] *Christopher J. Rekatas,*[2] *Shao-Min Mai,*[2] *David Attwood,*[2] *Colin Booth,**[2] *Anthony J. Ryan,*[3] *I. W. Hamley,*[4] *Luigi G. A. Martini*[5]

[1] National and Kapodistrian University of Athens, Department of Chemistry, Physical Chemistry Laboratory, Panepistimiopolis, 157 71 Athens, Greece
[2] Department of Chemistry and School of Pharmacy, University of Manchester, Manchester M13 9PL, UK
[3] Department of Chemistry, University of Sheffield, Sheffield S3 7HF, UK
[4] School of Chemistry, University of Leeds, Leeds LS2 9JT, UK
[5] SmithKline Beecham, New Frontiers Science Park (South), Harlow, Essex CM19 5AW, UK

Introduction

Copolymers comprising blocks of hydrophilic poly(oxyethylene) with hydrophobic poly(oxypropylene) or poly(oxybutylene) can micellise in dilute aqueous solution and their concentrated micellar solutions can form gels (liquid-crystal mesophases): see, for example, recent reviews[1–4] and papers.[5–7] Much of this research has been based on the availability of copolymers from commercial sources, although a broad program of preparative work has been carried out in Manchester.[1]

By comparison, little is known about the association behaviour of corresponding copolymers with a hydrophobic poly(oxyphenylethylene) block prepared from styrene oxide. A single triblock copolymer and a short series of

  1022-1352/2001/0805–1345$17.50+.50/0

three diblock copolymers have been prepared, and their association properties studied in aqueous solution by Mai et al.[8,9] The gel phases of the diblocks were explored, but not in detail.[9] This paper reports work on a fourth diblock copolymer, including study of its aqueous gels by rheometry. There is a body of work on diblock copolymers of ethylene oxide and styrene, which provides a useful source of results for comparison.[10–20]

The notation used in describing the chain units of the copolymers is:

E	oxyethylene	OCH_2CH_2
P	oxymethylethylene (oxypropylene)	$OCH_2CH(CH_3)$
B	oxyethylethylene (oxybutylene)	$OCH_2CH(C_2H_5)$
S	oxyphenylethylene	$OCH_2CH(C_6H_5)$
St	phenylethylene	$CH_2CH(C_6H_5)$

Thus a diblock copolymer of ethylene oxide and styrene oxide is denoted E_mS_n, where the subscripts *m* and *n* denote number-average block lengths in repeat units. The copolymers previously studied were triblock $S_4E_{45}S_4$ and diblocks $E_{50}S_{3.5}$, $E_{50}S_{5.1}$ and $E_{51}S_{6.5}$.

Based on studies of the micellisation of diblock copolymers, it has been shown that the three types of repeat unit (P, B and S) have significantly different hydrophobicities.[1,9] Relative to oxypropylene, and with an estimated uncertainty of ±20%, these rank:

$$P:B:S = 1:6:12$$

The hydrophobicity of a St repeat unit is similar to that of an S unit.[9]

The copolymer of present interest was prepared initially for a related study of drug solubilisation in micellar solutions.[21] It is denoted $S_{13}E_{60}$, but see the *Experimental Part* for details. The notation indicates that styrene oxide was polymerised first, followed by ethylene oxide. There is a practical advantage in this procedure, since it is easier to disperse a few grams of low-molar-mass poly(S) in a large amount of liquid ethylene oxide rather than the reverse. Any widening of the E-block length distribution caused by slow initiation in the second stage of polymerisation should be small for E_{60}.[22,23] As described below, the study included characterisation of the copolymer by gel permeation chromatography (GPC) and ^{13}C NMR, of the micelles by dynamic and static light scattering, and of the gels by rheometry.

Experimental Part

Preparation and Characterisation of the Copolymer

Copolymer $S_{13}E_{60}$ was prepared by sequential anionic polymerisation of styrene oxide followed by ethylene oxide. Apart from the reversed sequence of polymerisation, the procedure largely followed that described previously.[9] The monofunctional initiator was 2-(2-methoxyethoxy)ethanol activated by reaction with potassium metal (molar ratio OH/K ≈ 23). This meant that the S block was initiated by $CH_3(OCH_2CH_2)_2O^-$, and that a more exact formula for the copolymer would be $E_2S_{13}E_{60}$. However, in view of the high hydrophobicity of the S units, the E_2 termination of the S block should not unduly influence the micellisation of the copolymer, and the abbreviated formula, which stresses its diblock nature, is preferred. The copolymer was characterised by gel permeation chromatography (GPC) and ^{13}C NMR spectroscopy.

The GPC system consisted of three μ-Styragel columns (Waters Associates, nominal porosity from 500–10^4 Å) eluted by tetrahydrofuran (THF) at 20 °C. Samples were injected *via* a 100 mm^3 loop at concentration 2 $g \cdot dm^{-3}$, and their emergence was detected by differential refractometry. The flow rate was 1 $cm^3 \cdot min^{-1}$, monitored by use of an internal marker (dodecane). Calibration was done with poly(oxyethylene) samples of known molar mass. A second GPC system with *N*,*N*-dimethylacetamide at 65 °C as eluent was used to check the results. The GPC curves obtained for the copolymer had a narrow main peak with a minor peak at lower elution volume, consistent either with moisture introduced at the first stage of polymerisation giving rise to a proportion of triblock copolymer $E_{60}S_{26}E_{60}$, or, and more likely, with moisture introduced at the second stage giving rise to a proportion of homopoly(oxyethylene) E_{120}. Analysis showed the width of the molar mass distribution of the copolymer itself (i.e. the ratio of mass-average to number-average molar mass) to be $\overline{M}_w/\overline{M}_n \approx 1.03 \pm 0.01$. The proportion of impurity was estimated from relative areas to be approximately 13 wt.-%.

^{13}C NMR spectra were recorded by means of a Varian Unity 500 spectrometer operated at 125.5 MHz. Solutions were *ca.* 10 wt.-% in $CDCl_3$. Assignments were taken from previous work.[24] The integrals of the resonances from backbone and end group carbons were used to determine average composition (i.e. mole fraction E) and an absolute value of the number-average molar mass. Allowance was made for the different nuclear Overhauser enhancements of E and S units.[24] The excess of E ends terminated with hydroxyl groups over those terminated by methoxy groups was consistent with the presence of *ca.* 10 wt.-% homopoly(oxyethylene), similar to the amount estimated by GPC. Allowance was made for this material in calculating the composition (64 wt.-% E) and the number-average molar mass ($\overline{M}_n$ = 4290 ± 90 $g \cdot mol^{-1}$) of the diblock copolymer.

Light Scattering

All glassware was washed with condensing acetone vapour before use. Solutions were clarified by filtering through Millipore Millex filters (Triton free, 0.22 μm porosity) directly into the cleaned scattering cell.

Static light scattering (SLS) intensities were measured for solutions at temperatures in the range 20–50 °C by means of a Brookhaven BI 200S instrument with vertically polarised incident light of wavelength λ = 488 nm supplied by an argon ion laser operated at 500 mW. The intensity scale was calibrated against benzene. Dynamic light scattering (DLS) measurements were made under similar conditions by means of the instrument described above making use of a Brookha-

ven BI 9000 AT digital correlator. Usually measurements of scattered light were made at the angle $\theta = 90^\circ$ to the incident beam. Experiment duration was in the range 5–20 min, and each experiment was repeated two or more times.

The correlation functions from dynamic light scattering (DLS) were analysed by the constrained regularised CONTIN method[25] to obtain distributions of decay rates (Γ). The decay rate distributions gave distributions of apparent diffusion coefficient ($D_{app} = \Gamma/q^2$, $q = (4\pi n/\lambda)\sin(\theta/2)$, n = refractive index of water) and hence of apparent hydrodynamic radius($r_{h,app}$, radius of the hydrodynamically equivalent hard sphere corresponding to D_{app}) via the Stokes-Einstein equation (Equation (1))

$$r_{h,app} = kT/(6\pi\eta D_{app}) \quad (1)$$

where k is the Boltzmann constant and η is the viscosity of water at temperature T.

The basis for analysis of static light scattering (SLS) was the Debye equation (Equation (2)) in the form

$$K^*c/(I-I_S) = 1/\bar{M}_w + 2A_2c + ... \quad (2)$$

where I is intensity of light scattering from solution relative to that from benzene, I_S is the corresponding quantity for the solvent, c is the concentration, $\bar{M}_w$ is the mass-average molar mass of the solute, A_2 is the second virial coefficient (higher coefficients being neglected) and K^* is the appropriate optical constant, which includes the specific refractive index increment, $\nu = dn/dc$.

Values of ν and its temperature increment were determined by means of an Abbé 60/ED precision refractometer (Bellingham and Stanley). Values of 0.157 $cm^3 \cdot g^{-1}$ at 20 °C and 2×10^{-4} $cm^3 \cdot g^{-1} \cdot K^{-1}$ satisfactorily represented the data. Sources of the other quantities necessary for calculating K^* have been given previously.[26] The effect of different refractive indices of the blocks on the derived molar masses of copolymers of this type has been considered previously and found to be small.[8, 9]

Preparation of Gels

Solutions were prepared by weighing copolymer and water into small tubes and mixing, if possible, in the high-temperature mobile state before being stored for a day or more at low temperature ($T \approx 5$ °C). Otherwise the mixture was allowed to mix by diffusion over a period of days at 5 °C. Newly prepared samples were used for each experiment.

Rheometry

The rheological properties of the samples were determined using a Bohlin CS50 Rheometer with water-bath temperature control. Couette geometry (bob, 24.5 mm diameter, 27 mm height; cup, 26.5 mm diameter, 29 mm height) was used, with 2.5 cm^3 sample being added to the cup in the mobile state. A solvent trap maintained a water-saturated atmosphere around the cell, and evaporation was not significant for the temperatures and time scales investigated.

Storage and loss moduli were recorded across the temperature range with the instrument in oscillatory-shear mode at a frequency of 1 Hz. In this mode, the samples were heated at 1 °C · min^{-1} in the range 5–95 °C. Also, moduli were measured with the gels at fixed temperature across the frequency range 0.003 to 30 Hz. For all measurements the strain amplitude was low (<0.5%, linear viscoelastic region), thus ensuring that G' and G'' were independent of strain.

Measurements of yield stress and viscosity were made at selected temperatures with the instrument in continuous-shear mode. The instrument was programmed to increase the shear stress in a series of logarithmically-spaced steps, allowing 1 min to reach equilibrium at each step. Usually a period of 20 min was allowed for temperature equilibration before starting the program.

In related tube-inversion experiments, carried out as described previously,[9] samples (0.5 g) were enclosed in small tubes (internal diameter *ca.* 10 mm), and observed whilst slowly heating (or cooling) the tube in a water bath within the range 0–85 °C. The heating/cooling rate was 0.5 °C · min^{-1}. The change from a mobile to an immobile system (or vice-versa) was determined by inverting the tube.

Results

No clouding was observed: i.e. all solutions investigated (0.2 to 65 wt.-%) remained clear to the eye over the temperature range 5–85 °C.

Hydrodynamic Radius

Dynamic light scattering (DLS) measurements were made on solutions in the concentration range 2 to 27 g · dm^{-3} at 20, 30 and 40 °C. Intensity fraction distributions of the logarithm of apparent hydrodynamic radius found for the solutions at 20 °C are illustrated in Figure 1. The peaks at $r_{h,app} \approx 10$ nm are characteristic of micelles. Similar, rather narrower, distributions were found for the micellar solutions at the higher temperatures. Reciprocal intensity-average apparent hydrodynamic radii, calculated in the CONTIN program, are plotted against concentration in Figure 2. Note that through Equation (1), the reciprocal of $r_{h,app}$ is proportional to $D_{app}\eta/T$ and so, compared to D_{app}, is compensated for changes in solvent viscosity and temperature. The values of r_h obtained by extrapolation to zero concentration are very similar (range 9.5–9.8 nm, see Table 1). The insensitivity of r_h to temperature in micellar systems of this type has been discussed many times previously, as has the positive slope of plots like Figure 2 (or the corresponding plots of D_{app} *versus* c), which signifies effective hard-sphere behaviour. References can be found in cited reviews.[1, 2]

Association Number and Thermodynamic Radius

Static light scattering (SLS) measurements were made over a similar range of concentration and temperature: see Figure 3. The curvature of the plots means that Equa-

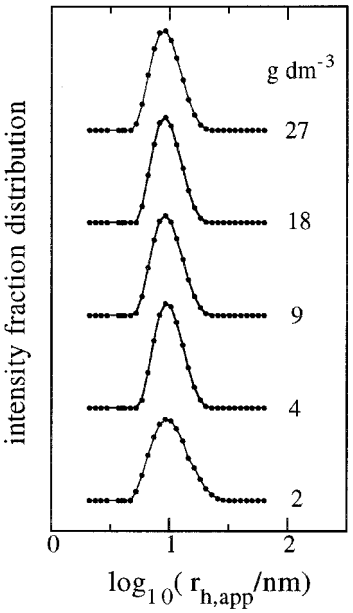

Figure 1. Dynamic light scattering. Intensity fraction distribution of the logarithm of apparent hydrodynamic radius for aqueous solutions of copolymer $S_{13}E_{60}$ at 20 °C and the concentrations (g · dm^{-3}) indicated.

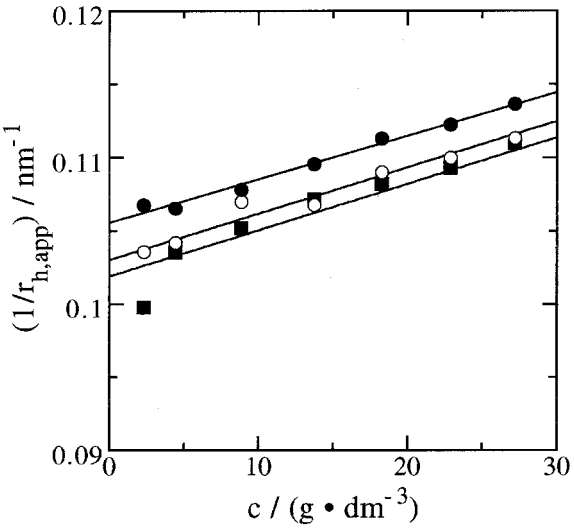

Figure 2. Dynamic light scattering. Reciprocal of apparent hydrodynamic radius *versus* copolymer concentration for aqueous solutions of copolymer $S_{13}E_{60}$ at (■) 20 °C, (○) 30 °C and (●) 40 °C.

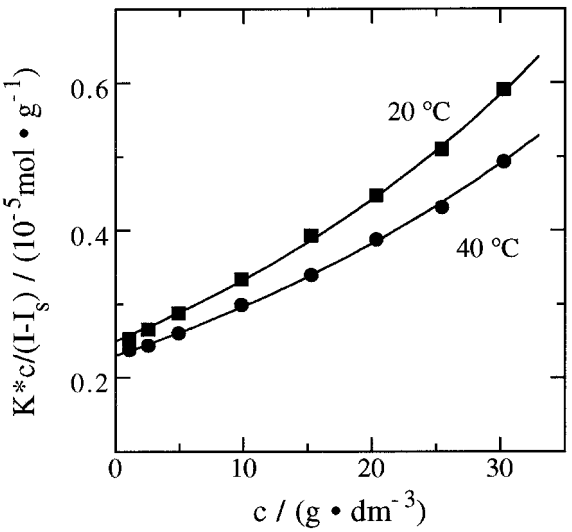

Figure 3. Static light scattering. Debye plots for aqueous solutions of copolymer $S_{13}E_{60}$ at the temperatures indicated. The curves were calculated using theory for hard spheres.[24] For clarity, similar data for solutions at 30 °C are not shown.

tion (2) must be expanded to include at least the third virial coefficient. In fact the curve shown is based on a modification of Percus-Yevick hard-sphere theory[27–29] which we have found useful for micellar solutions of a wide range of copolymers.[1, 6, 9, 30] The calculations require the density of anhydrous copolymer, i.e. $\rho_a \approx 1.13$ g · cm^{-3} calculated from the densities of the component polymers.[31–33] The intercept at $c = 0$ is the reciprocal mass-average micellar molar mass ($\overline{M}_w$) while the slope and curvature determine the average excluded volume of equivalent hard-sphere micelles (u), from which an effective hard-sphere volume can be calculated as $v_t = u/8$, and thereby a hard-sphere radius. Since the excluded volume is an equilibrium effect, this quantity is referred to as the thermodynamic radius r_t, as distinct from the hydrodynamic radius r_h. Specifically, the quantity derived was the thermodynamic expansion factor defined as $\delta_t = v_t/v_a$, where v_a is the anhydrous volume of a micelle calculated from $\overline{M}_w$ and ρ_a.

Values of $\overline{M}_w$, corrected for the impurity assuming 10 wt.-% homopoly(oxyethylene), are listed in Table 1, together with values of the mass-average association number,

$$N_w = \overline{M}_w \text{ (micelle)}/\overline{M}_w \text{ (copolymer)}$$

where $\overline{M}_w$ (copolymer) = 4420 g · mol^{-1}, calculated from $\overline{M}_n$ = 4290 g · mol^{-1} and $\overline{M}_w/\overline{M}_n$ = 1.03. Also listed are the thermodynamic expansion factor and the corresponding value of r_t obtained from $\delta_t = v_t/v_a$.

Phase Diagram

Tube-inversion experiments were used to define the immobile-gel region of the phase diagram. Immobility in this test requires the gel to have a yield stress higher than a critical value dependent on the conditions of the test. In the procedure described in the *Experimental Part*, the yield stress must be higher than *ca.* 40 Pa.[7] The resulting phase diagram is shown in Figure 4: the curve extending down to 0 °C reflects the fact that a 20 wt.-% solution was immobile at that temperature but a 19 wt.-% solution was

Table 1. Micelle properties for copolymer $S_{13}E_{60}$ in aqueous solution. Results from dynamic and static light scattering. D = diffusion coefficient; r_h = hydrodynamic radius; $\overline{M}_w$ = mass-average molar mass; N_w = mass-average association number; r_t = thermodynamic radius; δ_t = thermodynamic expansion factor. Estimated errors: ±10% in $\overline{M}_w$, N_w and δ_t, ±5% in D, r_h and r_t.

$\frac{T}{°C}$	$\frac{D}{10^{-11}\ m^2 \cdot s^{-1}}$	$\frac{r_h}{nm}$	$\frac{\overline{M}_w}{10^5\ g \cdot mol^{-1}}$	N_w	$\frac{r_t}{nm}$	δ_t
20	2.2	9.8	4.5	102	8.6	4.1
30	2.9	9.7	4.7	106	8.7	4.0
40	3.7	9.5	4.9	111	8.5	3.6

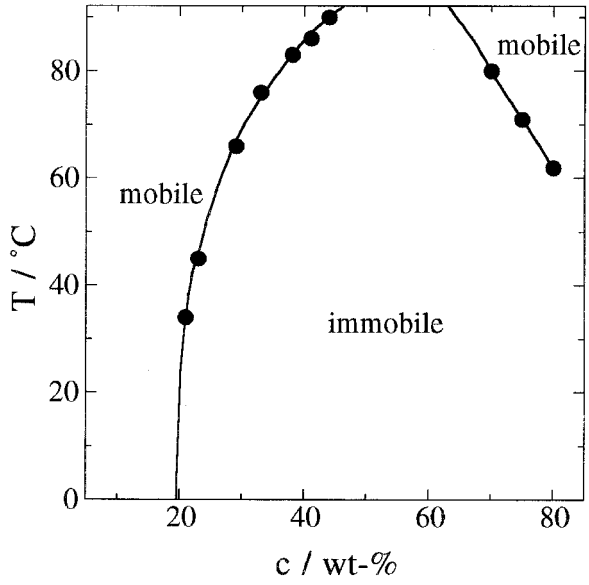

Figure 4. Phase diagram from tube inversion for aqueous solutions of copolymer $S_{13}E_{60}$.

not. Adopting the notation used by Hvidt et al.,[34] the immobile phase is referred to as 'hard gel'.

Effect of Temperature on Modulus

Selected plots of storage and loss moduli against temperature are shown in Figure 5 for aqueous solutions of concentration 4.0–19.6 wt.-%, i.e. below the hard-gel limit of *ca.* 20 wt.-%, see Figure 4. In all, eight solutions were examined in this range. The frequency used was 1 Hz. As seen in Figure 5, sols at low temperature ($G' < G''$ where distinguishable) transform to gels at high temperature ($G' > G''$). Since these gels are mobile in the tube-inversion test, these are 'soft' gels in Hvidt's notation.[34] The maximum value of the storage modulus of the soft gel increases with increase in copolymer concentration from *ca.* 30 Pa (4 wt.-%) to 550 Pa (19.6 wt.-%), while the temperature of first formation falls from 80 °C to 23 °C. The regions of sol and soft gel, as they relate to the hard-gel region, are shown in Figure 6. The effect of frequency on the sol/soft-gel boundary was not investigated: measurements on related systems confirm, as would be expected, that sol/soft-gel temperatures are lowered when frequency is increased.[7]

Corresponding modulus-temperature curves obtained for the hard gel region at higher concentrations (20–65 wt.-%) are illustrated in Figure 7. The temperature range was 5–90 °C. Not shown in Figure 7 are results obtained for a 50 wt.-% sample, which had a high storage modulus dropping from 20 to 3 kPa across the whole temperature range, and those for a 40 wt.-% sample, which had a storage modulus of similar magnitude but which started to fall away just before the high-temperature limit of the experiment. The sharp falls in modulus coincide with the hard gel boundary, as illustrated in Figure 6. For solutions of concentration below 45 wt.-%, these transitions were

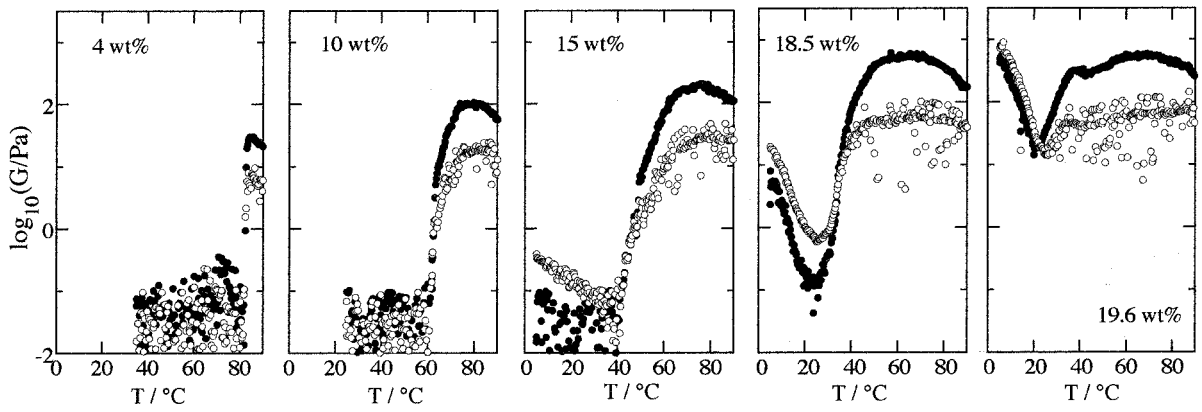

Figure 5. Temperature dependences of logarithmic storage and loss moduli (f = 1 Hz) for aqueous solutions of copolymer $S_{13}E_{60}$. Filled symbols denote $\log(G')$ and unfilled symbols denote $\log(G'')$. Copolymer concentrations (wt.-%) are indicated: all lie in the soft-gel range.

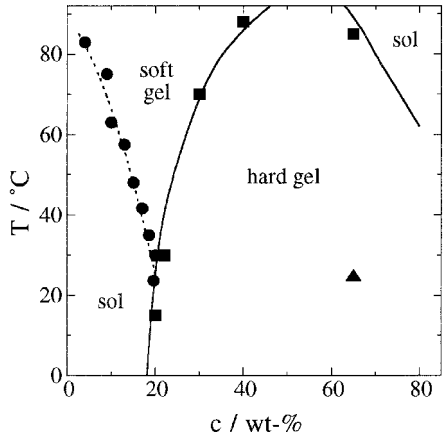

Figure 6. Phase diagram for aqueous solutions of copolymers $S_{13}E_{60}$. The solid curve is that defined for hard gel taken from Figure 4. Data points (●) and the dotted curve indicate the sol/soft-gel boundary; data points (■) indicate the temperatures at which the storage and loss moduli fell sharply to reach a low value, giving a coincident definition of the hard-gel boundary; data point (▲) indicates the temperature of a transition within the hard-gel region.

to soft gels, i.e. to phases which are mobile in the tube-inversion test but have $G' > G''$. The curve of the 65 wt.-% sample shows a transition at *ca.* 25 °C, and a second one at *ca.* 85 °C which coincides with the hard-gel boundary. In this case, the high-T phase formed is a sol.

In related experiments on aqueous micellar systems, for example on micellar solutions of copolymer $E_{22}B_7$,[35] gels with high storage modulus have been assigned to cubic phases formed from packed spherical micelles with body-centred symmetry by means of small-angle X-ray scattering experiments, while lower-modulus gels formed on increasing the temperature were similarly assigned to packed cylindrical micelles with hexagonal symmetry. It is possible that the low-T transition has a similar origin, but this can only be certain when structural information is available.

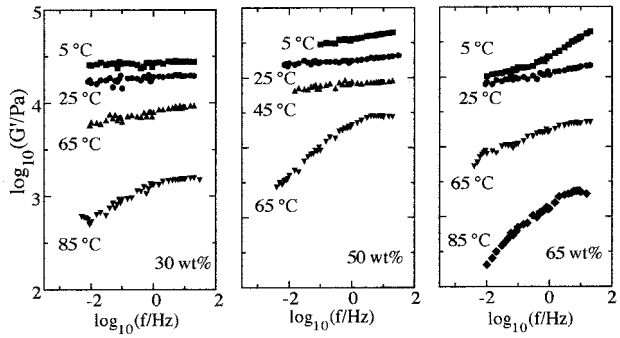

Figure 8. Frequency dependences of logarithmic storage moduli for aqueous solutions of copolymer $S_{13}E_{60}$. Copolymer concentrations (wt.-%) and solution temperatures (°C) are indicated. At 85 °C, the 30 wt.-% solution is in the soft-gel region, and the 65 wt.-% solution is at the hard-gel/sol boundary (see Figure 6): otherwise the solutions lie in the hard-gel region.

The experiments included a brief study of the effect of frequency (0.003–30 Hz) on modulus of gels within the hard gel range (22–65 wt.-%). As examples, plots of G' against $\log(f)$ for 30, 50 and 65 wt.-% gels are shown in Figure 8. For the 30 wt.-% gel, G' was not greatly dependent on frequency at temperatures well below the hard-gel/soft-gel boundary (5 and 25 °C), which is consistent with a cubic gel.[7,36,37] Above the boundary (85 °C, soft gel) G' varied significantly with frequency. Similar results were obtained for other gels with concentrations in the range 22–40 wt.-%. The 50 wt.-% gel showed similar behaviour at low temperatures (5–45 °C), but at 65 °C (i.e. well below the hard-gel/soft-gel boundary - see Figure 6) G' was dependent on frequency. However, it reached its plateau value at or about 1 Hz. At 25 and 65 °C the 65 wt.-% sample behaved similarly to the 50 wt.-%. At 85 °C the 65 wt.-% sample is at the hard-gel/sol boundary, and frequency dependent moduli might be expected. The behaviour of the 65 wt.-% hard gel at 5 °C was anomalous: without doubt this is related to the transi-

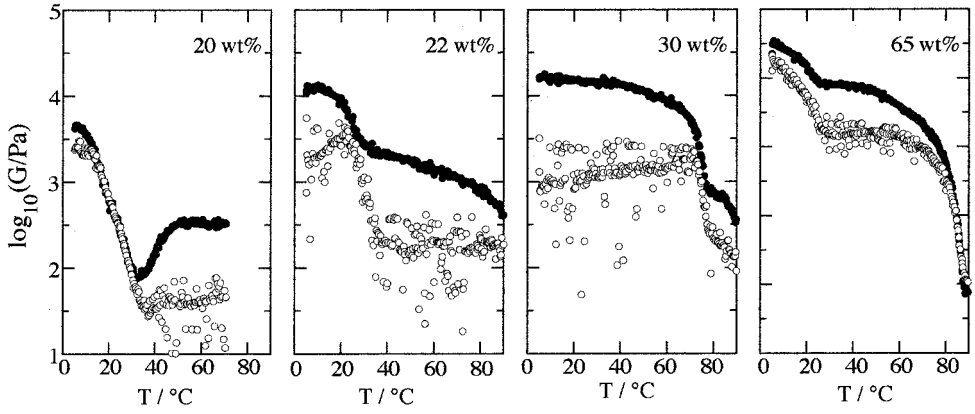

Figure 7. Temperature dependencies of logarithmic storage and loss moduli (f = 1 Hz) for aqueous solutions of copolymer $S_{13}E_{60}$. Filled symbols denote $\log(G')$ and unfilled symbols denote $\log(G'')$. Copolymer concentrations (wt.-%) are indicated: all lie in the hard-gel range.

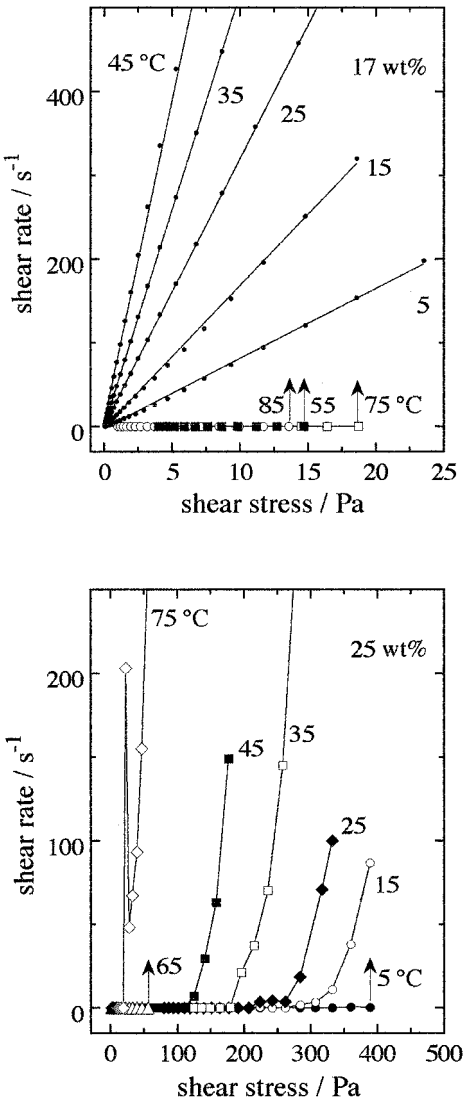

Figure 9. Shear rate *versus* shear stress for aqueous solutions of copolymer $S_{13}E_{60}$ (continuous-shear mode). Copolymer concentrations (wt.-%) and solution temperatures (°C) are indicated. The 17 wt.-% sample is a soft gel at 55–85 °C and a sol at lower temperatures. The 25 wt.-% sample is a soft gel at 75 °C and a hard gel at lower temperatures. The arrows indicate catastrophic yield of the gel.

tion seen in the $G'(T)$ curve of this sample at low temperatures (see Figure 7). Overall, the evidence for the hard gels is that values of the storage modulus measured at 1 Hz are essentially plateau values, i.e. they approximate the limiting value of G'_∞.

Yield Stress

The plots of shear rate against shear stress for 17 wt.-% and 25 wt.-% solutions at various temperatures shown in Figure 9 are representative of results obtained in the soft-gel and hard-gel regions of the phase diagram. The 17 wt.-% sample formed soft gels at high temperature (55–85 °C, see Figure 6) which yielded at shear stresses less than 20 Pa. The sols at lower temperatures had zero yield stress and Newtonian viscosities (0.12 to 0.013 Pa · s at 5 to 45 °C). The 25 wt.-% sample formed hard gels at temperatures below 60 °C (see Figure 6) which yielded at high shear stresses (120–400 Pa) to form shear-thinning fluids. At 75 °C the sample was a soft gel which eventually yielded at low shear stress (*ca.* 18 Pa) and, after some complexity, formed a shear-thinning fluid.

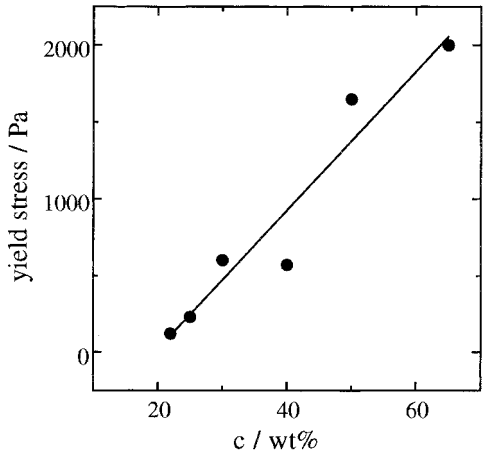

Figure 10. Concentration dependence of yield stress for aqueous solutions of copolymer $S_{13}E_{60}$ at 25 °C. The data cover the hard gel region.

Figure 10 shows yield stresses obtained for hard gels at 25 °C over a range of copolymer concentrations. Within the considerable scatter, the yield stresses increase linearly with increase in copolymer concentration.

Discussion

Micelle Properties

The micelle association number obtained for copolymer $S_{13}E_{60}$ is compared with values obtained previously for $E_{50}S_n$ copolymers with shorter S blocks in Figure 11a, where the values are for solutions at 40 °C. As can be seen, a linear relationship holds when N_w is plotted against the hydrophobe block length (n), with the intercept at $N_w = 0$ indicating a critical block length for micellisation of $n_{cr} \approx 1$ S unit when the E-block is 50–60 units long. This value can be compared with reported values of $n_{cr} \approx 4$ B units (for E_{30}) and $n_{cr} \approx 28$ P units (for E_{100}).[1]

Log-log plots of N_w, r_t and r_h against n-n_{cr} are shown in Figure 11b. The slopes of the plots are recorded in Table 2, where they are compared with those derived in a parallel way for related E_mB_n and E_mP_n diblock copolymers.[1] There is good agreement between the experimental results for the three systems: i.e. using the standard error

$$N_w \sim n^{1.05\pm0.06} \quad r_t \sim n^{0.48\pm0.05} \quad r_h \sim n^{0.21\pm0.01}$$

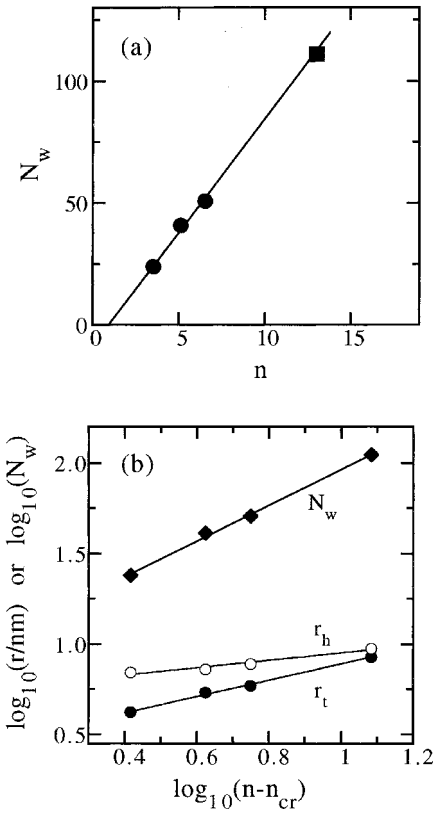

Figure 11. (a) Micelle association number (N_w) *versus* hydrophobe block length (n, *S* units) for solutions of (●) $E_{50}S_n$ (ref.[9]) and (■) $S_{13}E_{60}$ at 40 °C. (b) Corresponding log-log plots of association number (N_w), hydrodynamic radius (r_h) and thermodynamic radius (r_t) (as indicated) against n-n_{cr}, where n_{cr} is the critical hydrophobe length for micelle formation taken from plot (a). The slopes of the lines through the points are listed in Table 2.

Table 2. Scaling exponents for micelles of diblock copoly(oxyalkylene)s in aqueous solution.

Copolymers	T / °C	Range of n	slope		
			N_w	r_t	r_h
$E_{50-60}S_n$	40	3.5–13	0.99	0.45	0.20
$E_{27-32}B_n$	30	5–14	1.17	0.58	0.20
$E_{92-104}P_n$	35	37–73	0.98	0.41	0.22

The results can be compared with theoretical predictions of the scaling exponents, which lie in the range 0.9–1.2 for association number and 0.06–0.16 for radius.[3, 38–44] The theoretical work relates to radius of gyration, and cannot be expected to predict the result for the thermodynamic radius which originates in the excluded volume. The hydrodynamic radius is more closely related to the radius of gyration, and the scaling exponent (0.21) at least approaches the range of the theoretical values.

The micelle properties of diblock copolymers of styrene and ethylene oxide in aqueous solution have been

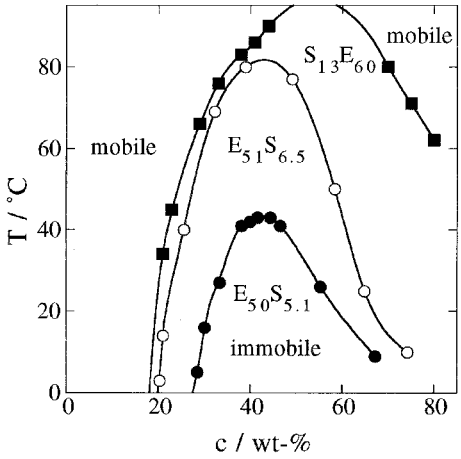

Figure 12. Phase diagrams from tube inversion for aqueous solutions of (■) $S_{13}E_{60}$ (present work) and (○) $E_{51}S_{6.5}$ and (●) $E_{50}S_{5.1}$ (ref.[9]).

reported from a number of laboratories covering a wide range of concentrations.[10–20] Of these, results for copolymer $St_{10}E_{68}$ are most readily compared with present results for $S_{13}E_{60}$. Unfortunately, values of the association number reported for micelles of $St_{10}E_{68}$ in water at ambient range from 60 to over 400.[14, 17, 20] Very high values may derive from the presence of large particles, as frequently reported for samples of E/St block copolymers in dilute aqueous solution.[11, 13, 20] The lowest value[20] is from sedimentation velocity and so independent of a second population of particles. However the discrepancies remain to be resolved. Here we note that the value of $N_w \approx 100$ obtained for copolymer $S_{13}E_{60}$ in solution at 20 °C lies within the 60–400 range. The result is consistent with our previous conclusion,[9] based on consideration of critical micelle concentrations, that the hydrophobicities of phenylethylene (St) and oxyphenylethylene (S) chain units are similar.

Gelation and Gel Properties

The hard gel boundaries found for E/S copolymers are compared in Figure 12. Solutions of copolymer $S_{3.5}E_{50}$ do not form a hard gel at any concentration and temperature. Corresponding phase diagrams for St_nE_m copolymers have not been reported.

The increase in high-T stability with increase in hydrophobe block length (seen in Figure 12) is typical of hard gels formed from copolymers of this type: see also, for example, the phase diagrams reported for aqueous solutions of E_mB_n diblock copolymers in Figure 10 of ref.[35] High-T destabilisation of hard gel in triblock copolymer ($E_mP_nE_m$) systems has been assigned on experimental grounds[34, 45] (with some support from theory)[46] to a spherical-to-cylindrical micellar transition, with consequent release of packing constraints. It is known that the

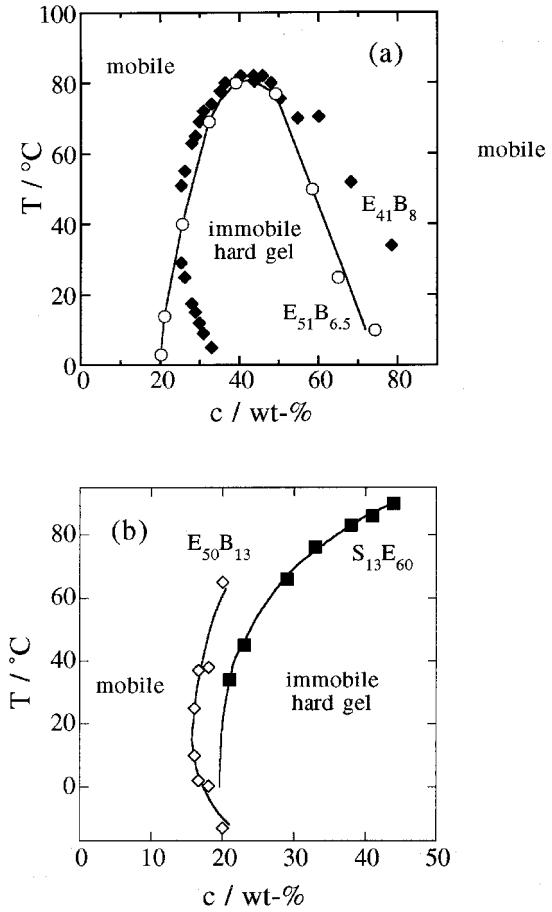

Figure 13. Comparison of phase diagrams from tube inversion for aqueous solutions of E/S and E/B block copolymers (B = oxybutylene): (a) (○) $E_{51}S_{6.5}$ (ref.[9]) and (♦) $E_{41}B_8$: (b) (■) $S_{13}E_{60}$ (present work) and (◇) $E_{50}B_{13}$ (ref. [50]).

association numbers of present and related block-copolymer micelles increase with temperature (see Table 2, also ref.[5, 47]). Considering a simple model of spherical micelles with anhydrous cores, the core radius increases as $N^{1/3}$ and the loss of conformational entropy related to stretching of a short hydrophobe block when N is large can destabilise spherical micelles in favour of cylindrical micelles. Conversely, if the hydrophobe block is long, the stretching effect is relatively small and spherical micelles are stable. The argument holds equally well for water-swollen cores: in this case the enhanced effect caused by swelling is only partly compensated by expulsion of water as the solvent quality reduces with increase in temperature.

The gelation behaviours of aqueous micellar solutions of E/S and E/B diblock copolymers are compared in Figure 13. Hard-gel boundaries of $S_{6.5}E_{51}$[9] and $E_{41}B_8$[48] in the range 20–80 wt.-% copolymer are shown in Figure 13a. Overall the two phase diagrams are similar. However, an important difference lies in the low-concentration range where $E_{41}B_8$ solutions gel on heating, the so-called cold gelation effect,[49] but $S_{6.5}E_{51}$ solutions do not. The data are not available for a similar comparison for $S_{13}E_{60}$ over a full concentration range, but a similar pattern is seen at low concentrations if comparison is made with results for solutions of copolymer $E_{50}B_{13}$: see Figure 13b. The mechanism of cold gelation has been discussed at length elsewhere.[6, 50] A number of factors combine to produce the effect: the micelle-molecule equilibrium, the negative temperature coefficient of solubility of the molecules, and modification of the hydrogen-bonded structure of water in concentrated poly(oxyethylene) solution. The effect is disrupted by any factor which stabilises micelles at low temperature, whether thermodynamic (e.g. crystallisation of blocks in the micelle core)[51] or kinetic (glass formation in the core).[14, 19, 52] In the present case of E/S copolymers neither of these proven explanations obviously applies: the S block is atactic[24] so crystallisation is not a factor, while the glass transition temperature of high-molar-mass poly(styrene oxide) is only 40 °C[33] and will be lower for the short block lengths under consideration. We hope to investigate this absence of cold gelation in the E/S-water system in future work.

A soft-gel region in the dilute concentration range of the phase diagram is as expected. In fact phase diagrams very similar to Figure 6 have been reported for dilute micellar solutions of a series of E_mB_n block copolymers with lengthy E blocks forming spherical micelles.[7] This type of soft-gel can be assigned to a percolation mechanism whereby structures of weakly-interacting spherical micelles form in the system. The transition from sol to soft gel is assumed to occur when micellar aggregates reach a percolation threshold yielding sufficient structure to cause an increase in modulus and, at a suitable frequency, the dynamic storage modulus to exceed the loss modulus.[7, 53, 54] More complex behaviour is expected if the micelles are subject to a sphere-to-cylinder transition,[34, 35] and the present results for the soft gel region are indicative of spherical micelles across the whole temperature range.

Acknowledgement: We thank Mr *S. K. Nixon* for help with the GPC experiments. The *Engineering and Physical Research Council* (UK) provided financial assistance for synthesis of block copolymers through grant GR/L22645. Cooperation between the Greek and UK groups was assisted by the *EU-TRM network* `Complex Architectures in Diblock Based Copolymer Systems'.

Received: May 15, 2000

[1] C. Booth, D. Attwood, *Macromol. Rapid Commun.* **2000**, *21*, 501.
[2] B. Chu, Z.-K. Zhou, in: "*NonionicSurfactants, Poly(oxyalkylene) Block Copolymers, Surfactant Science Series*", Vol. 60, V. M. Nace, Ed., Marcel Dekker, New York 1996, ch. 3.

[3] I. W. Hamley, "*The Physics of Block Copolymers*", Oxford U.P., Oxford 1998, ch. 3, 4.
[4] M. Almgren, W. Brown, S. Hvidt, *Colloid Polym. Sci.* **1995**, *273*, 2.
[5] G. Wanka, H. Hoffmann, W. Ulbricht, *Macromolecules* **1994**, *27*, 4145.
[6] L. Derici, S. Ledger, S.-M. Mai, C. Booth, I. W. Hamley, J. S. Pedersen, *Phys. Chem. Chem. Phys.* **1999**, *1*, 2773.
[7] A. Kelarakis, W. Mingvanish, C. Daniel, H. Li, V. Havredaki, C. Booth, I. W. Hamley, A. J. Ryan, *Phys. Chem. Chem. Phys.* **2000**, *2*, 2755.
[8] S.-M. Mai, S. Ludhera, F. Heatley, D. Attwood, C. Booth, *J. Chem. Soc., Faraday Trans.* **1998**, *94*, 567.
[9] S.-M. Mai, C. Booth, A. Kelarakis, V. Havredaki, A. J. Ryan, *Langmuir* **2000**, *16*, 1681.
[10] P. Bahadur, N. V. Sastry, *Eur. Polym. J.* **1988**, *24*, 285.
[11] R. Xu, M. A. Winnik, F. R. Hallett, G. Reiss, M. D. Croucher, *Macromolecules* **1991**, *24*, 87.
[12] M. Wilhelm, C.-L. Zhao, Y. Wang, R. Xu, M. A. Winnik, G. Reiss, M. D. Croucher, *Macromolecules* **1991**, *24*, 1033.
[13] R. Xu, M. A. Winnik, G. Riess, B. Chu, M. D. Croucher, *Macromolecules* **1992**, *25*, 644.
[14] A. Jada, G. Hurtrez, B. Siffert, G. Riess, *Macromol. Chem. Phys.* **1996**, *197*, 3697.
[15] P. Hickl, M. Ballauff, A. Jada, *Macromolecules* **1996**, *29*, 4006.
[16] P. Hickl, M. Ballauff, P. Lindner, A. Jada, *Colloid Polym. Sci.* **1997**, *275*, 1027.
[17] K. Mortensen, W. Brown, K. Almdal, E. Alami, A. Jada, *Langmuir* **1997**, *13*, 3635.
[18] P. F. Dewhirst, M. R. Lovell, J. L. Jones, R. W. Richards, J. R. P. Webster, *Macromolecules* **1998**, *31*, 7851.
[19] G. Hurtrez, P. Dumas, G. Riess, *Polym. Bull. (Berlin)* **1998**, *40*, 203.
[20] L. M. Bronstein, D. M. Chernyshov, G. I. Timofeeva, L. V. Dubrovina, P. L. Valetsky, A. R. Khokhlov, *Langmuir* **1999**, *15*, 6195.
[21] C. J. Rekatas, S.-M. Mai, M. Crothers, M. Quinn, F. Heatley, L. G. A. Martini, J. H. Collett, D. Attwood, *J. Pharm. Sci.*, submitted.
[22] V. M. Nace, R. H. Whitmarsh, M. W. Edens, *J. Am. Oil Chem. Soc.* **1994**, *71*, 77.
[23] G.-E. Yu, Z. Yang, M. Ameri, D. Attwood, J. H. Collett, C. Price, C. Booth, *J. Phys. Chem. B* **1997**, *101*, 4394.
[24] F. Heatley, G.-E. Yu, M. D. Draper, C. Booth, *Eur. Polym. J.* **1991**, *27*, 471.
[25] S. W. Provencher, *Makromol. Chem.* **1979**, *180*, 201.
[26] Z. Yang, Y.-W. Yang, Z.-K. Zhou, D. Attwood, C. Booth, *J. Chem. Soc., Faraday Trans.* **1996**, *92*, 257.
[27] J. K. Percus, G. J. Yevick, *J. Phys. Rev.* **1958**, *110*, 1.
[28] A. Vrij, *J. Chem. Phys.* **1978**, *69*, 1742.
[29] N. F. Carnahan, K. E. Starling, *J. Chem. Phys.* **1969**, *51*, 635.
[30] W. Mingvanish, S.-M. Mai, F. Heatley, C. Booth, D. Attwood, *J. Phys. Chem. B* **1999**, *103*, 11269.
[31] S.-M. Mai, C. Booth, V. M. Nace, *Eur. Polym. J.* **1997**, *33*, 991.
[32] R. J. Kern, *Makromol. Chem.* **1965**, *81*, 261.
[33] G. Allen, C. Booth, S. J. Hurst, F. Vernon, R. F. Warren, *Polymer* **1967**, *8*, 406.
[34] S. Hvidt, E. B. Jørgensen, W. Brown, K. Schillen, *J. Phys. Chem.* **1994**, *98*, 12320.
[35] W. Mingvanish, A. Kelarakis, S.-M. Mai, C. Daniel, Z. Yang, V. Havredaki, I. W. Hamley, A. J. Ryan, C. Booth, *J. Phys. Chem. B* **2000**, *104*, 9788.
[36] A. Kelarakis, V. Havredaki, L. Derici, G.-E. Yu, C. Booth, I. W. Hamley, *J. Chem. Soc., Faraday Trans.* **1998**, *94*, 3639.
[37] M. Portmann, E. H. Landau, P. L. Luisi, *J. Phys. Chem.* **1991**, *95*, 8437.
[38] [38a] E. B. Zhulina, T. M. Birshtein, *Vysokomol. Soedin.* **1985**, *27*, 511; [38b] E. B. Zhulina, T. M. Birshtein, *Polym. Sci. USSR (Engl. Transl.)* **1986**, *27*, 570.
[39] A. Halperin, *Macromolecules* **1987**, *20*, 2943.
[40] J. Noolandi, K. M. Hong, *Macromolecules* **1983**, *16*, 1443.
[41] M. D. Whitmore, J. Noolandi, *Macromolecules* **1985**, *18*, 657.
[42] T. L. Bluhm, M. D. Whitmore, *Can. J. Chem.* **1985**, *63*, 249.
[43] R. Nagarajan, K. Ganesh, *J. Chem. Phys.* **1989**, *90*, 5843.
[44] C. Wu, J. Gao, *Macromolecules* **2000**, *33*, 645.
[45] K. Zhang, A. Khan, *Macromolecules* **1995**, *28*, 3807.
[46] J. Noolandi, A.-C. Shi, P. Linse, *Macromolecules* **1996**, *29*, 5907.
[47] H. Altinok, S. K. Nixon, P. A. Gorry, D. Attwood, C. Booth, A. Kelarakis, V. Havredaki, *Colloid Surf. B* **1999**, *16*, 73.
[48] H. Li, G.-E. Yu, C. Price, C. Booth, E. Hecht, H. Hoffmann, *Macromolecules* **1997**, *30*, 1347.
[49] I. R. Schmolka, *J. Biomed. Mater. Res.* **1972**, *6*, 571.
[50] A. D. Bedells, R. M. Arafeh, Z. Yang, D. Attwood, J. C. Padget, C. Price, C. Booth, *J. Chem. Soc., Faraday Trans.* **1993**, *89*, 1243.
[51] P. R. Knowles, R. J. Barlow, F. Heatley, C. Booth, C. Price, *Macromol. Chem. Phys.* **1994**, *195*, 2555.
[52] S. Tanodekaew, J. Godward, F. Heatley, C. Booth, *Macromol. Chem. Phys.* **1997**, *198*, 3385.
[53] L. Lobry, N. Micali, F. Mallamace, C.Liao, S.-H. Chen, *Phys. Rev. E* **1999**, *60*, 7076.
[54] H. H. Winter, M. Mours, *Adv. Polym. Sci.* **1997**, *134*, 165.